

# VLM2Rec: Resolving Modality Collapse in Vision-Language Model Embedders for Multimodal Sequential Recommendation

Junyoung Kim  
Pohang University of  
Science and Technology  
Pohang, Republic of Korea  
junyoungkim@postech.ac.kr

Woojoo Kim  
Pohang University of  
Science and Technology  
Pohang, Republic of Korea  
kimuj0103@postech.ac.kr

Jaehyung Lim  
Pohang University of  
Science and Technology  
Pohang, Republic of Korea  
jaehyunglim@postech.ac.kr

Dongha Kim  
Pohang University of  
Science and Technology  
Pohang, Republic of Korea  
dhkim0317@postech.ac.kr

Hwanjo Yu\*  
Pohang University of  
Science and Technology  
Pohang, Republic of Korea  
hwanjoyu@postech.ac.kr

## Abstract

Sequential Recommendation (SR) in multimodal settings typically relies on small frozen pretrained encoders, which limits semantic capacity and prevents Collaborative Filtering (CF) signals from being fully integrated into item representations. Inspired by the recent success of Large Language Models (LLMs) as high-capacity embedders, we investigate the use of Vision-Language Models (VLMs) as CF-aware multimodal encoders for SR. However, we find that standard contrastive supervised fine-tuning (SFT), which adapts VLMs for embedding generation and injects CF signals, can amplify its inherent modality collapse. In this state, optimization is dominated by a single modality while the other degrades, ultimately undermining recommendation accuracy. To address this, we propose **VLM2Rec**, a VLM embedder-based framework for multimodal sequential recommendation designed to ensure balanced modality utilization. Specifically, we introduce *Weak-modality Penalized Contrastive Learning* to rectify gradient imbalance during optimization and *Cross-Modal Relational Topology Regularization* to preserve geometric consistency between modalities. Extensive experiments demonstrate that VLM2Rec consistently outperforms state-of-the-art baselines in both accuracy and robustness across diverse scenarios.

## CCS Concepts

• **Information systems** → **Recommender systems**.

## Keywords

Vision Language Models, Modality Collapse, Sequential Recommendation

\*Corresponding author

Permission to make digital or hard copies of all or part of this work for personal or classroom use is granted without fee provided that copies are not made or distributed for profit or commercial advantage and that copies bear this notice and the full citation on the first page. Copyrights for components of this work owned by others than the author(s) must be honored. Abstracting with credit is permitted. To copy otherwise, or republish, to post on servers or to redistribute to lists, requires prior specific permission and/or a fee. Request permissions from [permissions@acm.org](mailto:permissions@acm.org).

Conference acronym 'XX, Woodstock, NY

© 2026 Copyright held by the owner/author(s). Publication rights licensed to ACM.

ACM ISBN 978-1-4503-XXXX-X/2018/06

<https://doi.org/XXXXXXXX.XXXXXXX>

## ACM Reference Format:

Junyoung Kim, Woojoo Kim, Jaehyung Lim, Dongha Kim, and Hwanjo Yu. 2026. VLM2Rec: Resolving Modality Collapse in Vision-Language Model Embedders for Multimodal Sequential Recommendation. In *Proceedings of Make sure to enter the correct conference title from your rights confirmation email (Conference acronym 'XX)*. ACM, New York, NY, USA, 11 pages. <https://doi.org/XXXXXXXX.XXXXXXX>

## 1 Introduction

Sequential Recommendation (SR) models dynamic preferences from interaction histories [9, 14, 35, 48], yet ID-based methods struggle with data sparsity and cold-start issues. Incorporating auxiliary modalities (e.g., text, image) has become essential, providing richer item semantics that improve accuracy and generalization.

To leverage these modalities, existing approaches [12, 37, 43, 45] typically extract item features with small pretrained encoders [6, 30] and freeze them to maintain semantic integrity. However, this static approach creates a bottleneck: frozen embeddings cannot adequately internalize Collaborative Filtering (CF) dynamics, motivating a shift toward large-capacity models capable of encoding sequence-level behavior patterns.

In the NLP field, this shift has been established by repurposing LLMs as large reasoning encoders for representation learning [16–18, 36, 38] and by fine-tuning them with sequence–target supervision for adapting recommenders to inject sequence-level CF signals directly into the embedding space [8, 21, 41]. A natural next step is to extend this paradigm to multimodal SR using VLMs. However, existing research [27, 44] largely focuses on item-level semantics (single text or image input), missing the sequence-level behavior patterns essential to SR. Given the strong textual and multi-image reasoning ability of modern open-source VLMs [3, 20, 49], we initially attempted to fine-tune VLMs with sequence-level objectives to obtain CF-aware multimodal embeddings; however, we find that naively porting the LLM pipeline to VLMs introduces a critical **modality collapse**.

Prior studies [15, 32, 34] report that VLMs often exhibit *modality collapse* or *modality gap*, over-relying on a *strong* modality while underutilizing the *weak* one, thereby producing embeddings that underrepresent weaker modalities. We first examine whether modality imbalance can be mitigated at the fusion stage for a naive approach

by revisiting common VLM prompting strategies (Sec. 2.2.1). Internal fusion interleaves text and image tokens into a single sequence, relying on self-attention for implicit fusion, but attention often biases toward the dominant modality. External fusion encodes each modality independently and fuses them afterward (e.g., sum/concat). While it can prevent cross-modal interference at the input level, the model itself is inherently biased during the pretraining stage, leaving the weak modality already under-represented. Thus, the root cause lies in the unbalanced optimization path rather than the fusion strategy, necessitating objective-level interventions. Moreover, we identify the **Paradox of SFT**: standard contrastive supervised fine-tuning (SFT) [22, 26], which is essential for adapting VLMs to the recommendation task, counterintuitively exacerbates modality collapse, resulting in harm to recommendation performance (more details in Sec. 3).

Specifically, we observed that the model engages in *shortcut learning* [2, 15, 25] to minimize the loss, disproportionately relying on the easier-to-learn *strong modality*. Consequently, the weak modality receives insufficient gradient signals and largely loses its ability to push negative samples away. This optimization imbalance induces modality collapse directly in the representation space, leading to unequal contributions from the two modalities in downstream recommendation. In turn, this adaptation step paradoxically widens the modality gap, indicating the need for objective-level interventions to restore the weak modality’s discriminative power.

Building on these insights, we propose **VLM2Rec**, a VLM embedder-based framework for multimodal SR. Rather than extracting individual item features separately, our approach explicitly encodes the entire interaction histories as a single sequence input to high-capacity VLMs. This allows the model to capture dynamic behavioral patterns beyond static item features and directly internalizes these signals into the representation space. To address the CL-based SFT paradox, we introduce two novel objectives: First, *Weak-modality Penalized Contrastive Learning* ( $\mathcal{L}_{\text{WPCL}}$ ) dynamically identifies the user-adaptive weak modality during training and amplifies its contrastive penalty, enforcing discriminative negative separation. Second, to prevent this aggressive separation from distorting the semantic space for weak modality, we propose *Cross-modal Relational Topology Regularization* ( $\mathcal{L}_{\text{CRTTR}}$ ). This preserves geometric consistency by aligning relative sequence-item topology (e.g., neighbor/ranking structure) of the weak modality with that of the strong modality. Crucially, this design enables a balanced utilization of multimodal signals, ensuring that both textual and visual dynamics are effectively synthesized to produce discriminative, CF-aware representations through sequence-level SFT. Across diverse benchmarks, VLM2Rec consistently improves recommendation accuracy, confirming both its effectiveness and robustness.

Our contributions are as follows:

- To the best of our knowledge, we first propose a VLM-based multimodal sequence encoding framework for SR.
- We empirically reveal the paradox of SFT: standard contrastive fine-tuning amplifies modality collapse in VLMs by failing to optimize the weaker modality on SR datasets.
- We introduce two objective-level interventions that dynamically restore discriminative power and preserve geometric topology, achieving state-of-the-art performance.

## 2 Proposed VLM Embedder-based Framework in Sequential Recommendation

In this section, we introduce our proposed base setting for the VLM embedder-based framework in SR. This setting is used as the default configuration in all subsequent sections.

### 2.1 Problem Formulation

Let  $\mathcal{U}$  and  $\mathcal{I}$  denote the set of users and items, respectively. Each item  $i \in \mathcal{I}$  is associated with multimodal information: textual data  $t_i$  (e.g., title) and visual data  $v_i$  (e.g., product image). For each user  $u \in \mathcal{U}$ , we define the historical interaction sequence as  $S_u = [i_1, i_2, \dots, i_{|S_u|}]$ , sorted chronologically. The objective of sequential recommendation is to predict the next item  $i_{|S_u|+1}$  that the user is most likely to interact with, given the context  $S_u$ .

### 2.2 VLM-based Sequence Encoding

We utilize a pre-trained VLM, denoted as  $\Phi(\cdot)$ , as the backbone sequence encoder. Leveraging the multi-image understanding and context reasoning capabilities of the VLM, we extract sequence-level multimodal representations directly.

**2.2.1 Input Construction.** We compare the standard *Internal Fusion* (interleaved inputs) against our proposed *External Fusion* (separate inputs), defined as follows:

#### Interleaved Prompt (Internal)

Describe this item sequence in one word,

0) <|item1\_title|> <|item1\_image|>, ..., N) <|itemN\_title|>  
<|itemN\_image|>

#### Proposed Separate Prompts (External)

[ $P_T$ ]: Describe this item text sequence in one word,

0) <|item1\_title|>, ..., N) <|itemN\_title|>

[ $P_V$ ]: Describe this item image sequence in one word,

0) <|item1\_image|>, ..., N) <|itemN\_image|>

For *internal fusion*, text and images are processed simultaneously. In contrast, for *external fusion*, prompts  $P_T$  and  $P_V$  are input separately into the encoder to ensure independent encoding. Additionally, to extract individual item representations, we apply the same template but restrict the input to the first item placeholder (index 0).

**2.2.2 Representation Extraction.** Following standard conventions, we regard the hidden state of the last token from the VLM’s final transformer layer as the compressed semantic representation of the input. Given the text sequence  $S_u^T$  and visual sequence  $S_u^V$ , their corresponding sequence embeddings  $\mathbf{z}_u^T$  and  $\mathbf{z}_u^V$  are extracted as follows:

$$\mathbf{z}_u^T = \Phi(P_T(S_u^T)), \quad \mathbf{z}_u^V = \Phi(P_V(S_u^V)) \quad (1)$$

where  $\mathbf{z}_u^T, \mathbf{z}_u^V \in \mathbb{R}^d$ . Similarly, for a candidate item  $i$ , its text embedding  $\mathbf{e}_i^T$  and visual embedding  $\mathbf{e}_i^V$  are extracted using the same encoder  $\Phi$ .

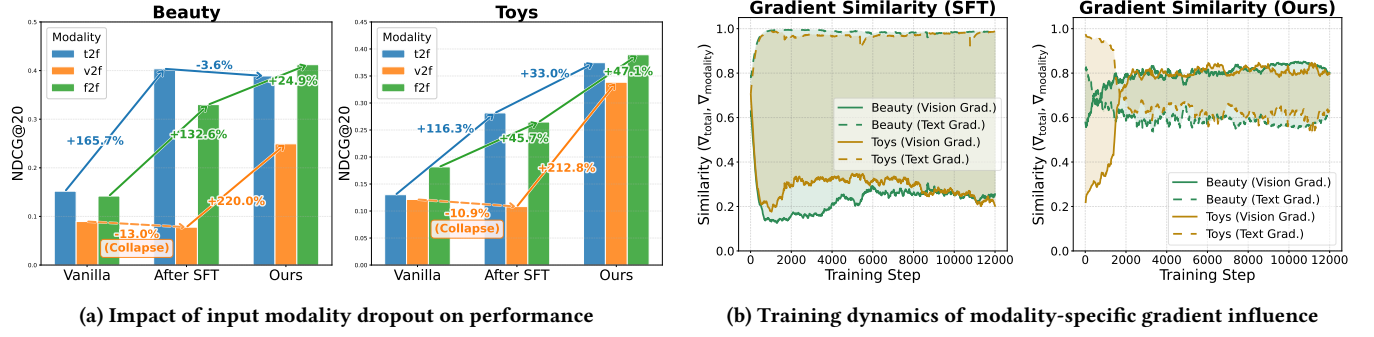


Figure 1: Analysis of modality collapse via dropout test and gradient dynamics. SFT makes the image modality act as a negative transfer when fused with text, because of the overlooked gradient signal of the weak modality during training. Our proposed VLM2Rec successfully re-balances modality gradients, enabling stable multimodal gains.

### 2.3 Fusion Strategy

Our primary goal is to balance modality influence through *objective-level* training signals, rather than introducing complex fusion strategies. To avoid additional parameters and improve generality, we use the simplest external fusion: element-wise summation,

$$\mathbf{z}_u = \mathbf{z}_u^T + \mathbf{z}_u^V, \quad (2)$$

and likewise fuse candidate item representations as  $\mathbf{e}_i = \mathbf{e}_i^T + \mathbf{e}_i^V$ .

### 2.4 Standard Supervised Fine-Tuning Objective

To adapt generative VLMs for retrieval and inject sequence-level CF signals, we employ conventional Supervised Fine-Tuning (SFT) via the InfoNCE loss [22, 26]. This objective aligns the representation space by maximizing the similarity between the user sequence  $\mathbf{z}_u$  and the positive item  $\mathbf{e}_{i^+}$  while distancing negatives:

$$\mathcal{L}_{\text{SFT}} = - \sum_{u \in \mathcal{B}} \log \frac{e^{s(\mathbf{z}_u, \mathbf{e}_{i^+})/\tau}}{e^{s(\mathbf{z}_u, \mathbf{e}_{i^+})/\tau} + \sum_{i^- \in \mathcal{N}_u} e^{s(\mathbf{z}_u, \mathbf{e}_{i^-})/\tau}} \quad (3)$$

where  $s(\cdot, \cdot)$  denotes cosine similarity,  $\tau$  is the temperature, and  $\mathcal{N}_u$  is the negative set.

## 3 The Paradox of SFT: Analysis of Modality Collapse in Sequential Recommendation

In this section, we present converging evidence of the **Paradox of SFT**: when adapting VLMs as embedders for SR, their objective function can worsen modality imbalance. We demonstrate this via i) *recommendation performance*, ii) *optimization dynamics*, and iii) *representation geometry* (Fig. 1, Tab. 1). The implementation follows in Sec. 2.

**Performance Gap and Negative Transfer** In Fig. 1a, to disentangle modality contributions in recommendation performance, we evaluate three sequence input settings for predicting the fused target:  $f2f$  (fused),  $t2f$  (text-only), and  $v2f$  (vision-only). In the Vanilla,  $v2f$  is consistently worst across datasets, revealing an intrinsic modality gap in pretrained VLMs for SR. Before fine-tuning, images can be either helpful or noisy depending on the dataset (e.g.,  $f2f$  drops on Toys but rises on Beauty). Crucially, after SFT the gap widens: while  $t2f$  and  $f2f$  improve,  $v2f$  performance degrades below even its Vanilla baseline; moreover,  $t2f$  consistently outperforms

$f2f$ . This confirms that standard SFT triggers negative transfer from the weak (vision) modality, acting as noise that compromises the fused embedding space.

**Optimization Dynamics** To investigate the cause, we track optimization dynamics by measuring the cosine similarity between the multimodal update  $\mathbf{g}_{\text{total}}$  and individual modality gradients  $\mathbf{g}_m$  for  $m \in \{T, V\}$ , computed under fused and single-modality inputs, respectively (Fig. 1b). This alignment quantifies each modality’s contribution to the actual update direction. From the start,  $\mathbf{g}_{\text{total}}$  is strongly aligned with the text gradient  $\mathbf{g}_T$ , while alignment with the image gradient  $\mathbf{g}_V$  drops rapidly. As training proceeds,  $\cos(\mathbf{g}_{\text{total}}, \mathbf{g}_T)$  goes to 1, whereas  $\cos(\mathbf{g}_{\text{total}}, \mathbf{g}_V)$  peaks briefly and then steadily declines due to the accumulation of modality bias. This shows that the model minimizes the contrastive objective by relying on the easier text modality, thereby failing to optimize the

Dataset	State	Mod.	$A_{\text{pos}}$ ( $\downarrow$ )	$A_{\text{neg}}$ ( $\uparrow$ )	$U$ ( $\downarrow$ )	$S$ ( $\uparrow$ )
Beauty	Vanilla	Fused	0.4859	0.5024	-0.3984	1.0340
		Vision	0.1550	0.1561	-0.0237	1.0071
		Text	0.4568	0.4742	-0.3691	1.0381
	After SFT	Fused	0.8041	0.9577	-1.7969	1.1910
		Vision	0.5752	0.5752	-0.0398	<b>1.0000</b>
		Text	0.7932	0.9429	-1.7422	1.1887
Ours	Fused	0.8488	1.0075	-1.9921	1.1870	
	Vision	0.2624	0.3184	<b>-0.2031</b>	<b>1.2134</b>	
	Text	0.7891	0.9184	-1.6718	1.1639	
Toys	Vanilla	Fused	0.5155	0.5469	-0.4707	1.0609
		Vision	0.1548	0.1554	-0.0237	1.0039
		Text	0.4900	0.5230	-0.4453	1.0673
	After SFT	Fused	0.7225	0.8972	-2.2500	1.2418
		Vision	0.5172	0.5126	<b>-0.0039</b>	<b>0.9911</b>
		Text	0.5346	0.6672	-2.2188	1.2480
Ours	Fused	0.8185	0.9502	-1.7969	1.1609	
	Vision	0.4557	0.5264	<b>-0.5703</b>	<b>1.1551</b>	
	Text	0.6115	0.6860	-0.9335	1.1218	

Table 1: Comparison of the representation geometry metrics among three states of VLMs.  $A_{\text{pos}}$  and  $A_{\text{neg}}$  denote positive and negative alignment,  $U$  represents uniformity, and  $S = A_{\text{neg}}/A_{\text{pos}}$  indicates separability.

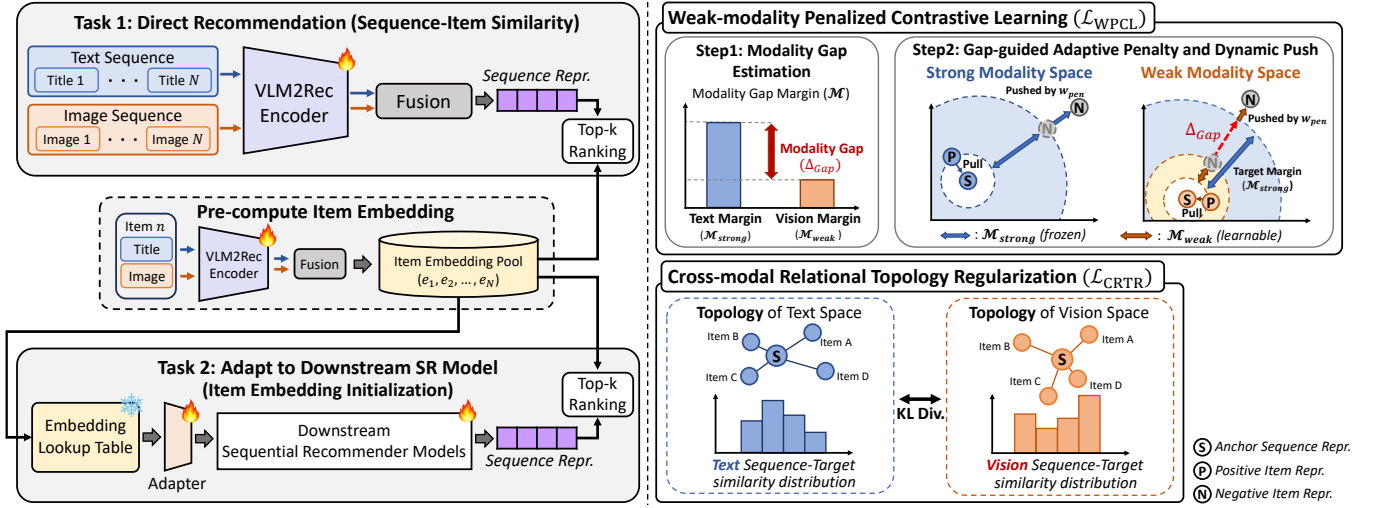


**Figure 2: Left: Our framework encodes text/image sequences/items to enable two usages: Task 1) direct sequence–item recommendation and Task 2) VLM2Rec-generated item embedding initialization for downstream SR models. Right: We fine-tune the VLM with  $\mathcal{L}_{WPCL}$  to adaptively penalize the user-specific weak modality (restoring negative separation) and  $\mathcal{L}_{CRTR}$  to align cross-modal relational topology, preventing geometric distortion while preserving modality individuality.**

visual modality to push negatives away and learn discriminative features.

**Geometric Analysis: Representation Collapse** To characterize how optimization bias translates into embedding geometry, we measure *alignment*  $A^m$  and *uniformity*  $U^m$ , widely used in representation learning [28, 39], for each modality  $m \in \{F, V, T\}$  (Tab. 1).

$$\begin{aligned}
 A_{pos}^m &\triangleq \mathbb{E}_{(s,i^+) \sim \mathcal{D}} \left[ \|\Phi_m(s) - \Phi_m(i^+)\|_2^2 \right], \\
 A_{neg}^m &\triangleq \mathbb{E}_{(s,i^+) \sim \mathcal{D}} \mathbb{E}_{i^- \sim \mathcal{P}_n(\cdot|s)} \left[ \|\Phi_m(s) - \Phi_m(i^-)\|_2^2 \right], \\
 U^m &\triangleq \log \mathbb{E}_{(s,i) \sim \mathcal{P}_u} \left[ \exp(-2\|\Phi_m(s) - \Phi_m(i)\|_2^2) \right].
 \end{aligned} \quad (4)$$

Here  $\mathcal{D}$  is the evaluation set of  $(s, i^+)$  pairs,  $\mathcal{P}_n(\cdot|s)$  is the negative sampler, and  $\mathcal{P}_u$  uniformly samples  $(s, i)$  pairs for estimating  $U^m$ .  $A_{pos}^m$  measures positive pull,  $A_{neg}^m$  measures negative push, and  $U^m$  reflects space coverage. We additionally define *separability* to capture the relative margin between negatives and positives.

$$S^m \triangleq \frac{A_{neg}^m}{A_{pos}^m + \epsilon}, \quad (5)$$

where  $S > 1$  indicates successful separation. In the Vanilla state, both modalities satisfy  $S > 1$ , but the fused geometry metrics ( $A^F, U^F, S^F$ ) already closely follow the text space, suggesting latent imbalance. After SFT, the text space improves as intended (better  $S^T, U^T$ ), whereas the vision space collapses:  $U^V$  changes only marginally on Beauty, but drops substantially on Toys, leading to near-indistinguishability ( $S \approx 1$  on Beauty) or even inversion ( $S < 1$  on Toys). Moreover,  $S^T > S^F$  across all settings implies that the under-optimized vision modality acts as noise, pulling the fused space toward the text-only trajectory. Overall, contrastive SFT amplifies intrinsic modality collapse in VLMs, degrading the weak modality’s separability and harming SR, which motivates

an objective-level design that explicitly restores weak-modality discrimination.

## 4 Method

In this section, we propose **VLM2Rec**, a novel multimodal SR framework designed to resolve the modality collapse observed in VLM-generated embeddings. Without auxiliary architectural complexity or sophisticated fusion modules, we aim to resolve this collapse through objective-level interventions.

### 4.1 Framework Design

Section 2 introduced the proposed VLM embedder-based SR framework. VLM2Rec adopts this foundational structure to ensure the consistency and generalizability of the proposed framework.

Specifically, VLM2Rec follows the minimal prompt construction in Section 2.2.1 to construct modality-specific inputs (text sequence and image sequence), and uses the same last-token representation extraction rule defined in Section 2.2.2 to extract sequence and item embeddings from the VLM. In addition, we inherit the element-wise summation fusion strategy from Section 2.3, which minimizes structural interference and avoids extra trainable parameters introduced for fusion. By adopting this proposed foundation, VLM2Rec maintains a simple architecture, enabling compatibility with publicly available off-the-shelf VLM backbones without requiring architecture-specific customization.

### 4.2 Training Objectives

**4.2.1 Weak-modality Penalized Contrastive Learning.** In Section 3, we reveal that standard contrastive objectives (Eq. 3) suffer from optimization imbalance in VLM-based embedders. This structurally marginalizes the weak modality, as the model satisfies the objective via shortcut learning on the strong modality without sufficiently

pushing negative samples in the weak modality’s representation space. A common method is to strengthen negatives at the data level (e.g., hard negative mining); however, such strategies introduce additional sophisticated sampling strategies. To overcome this limitation, we propose *Weak-modality Penalized Contrastive Learning* ( $\mathcal{L}_{\text{WPCL}}$ ).

*User-adaptive Modality Gap Estimation.* First, to quantify how clearly each modality discriminates the ground-truth item from negatives, we define the *Discriminative Margin*  $\mathcal{M}$ . Recognizing that users may differ in how much they rely on textual cues or visual cues in their purchasing behavior, we calculate this margin on a per-user basis.

For a user  $u$  and modality  $m \in \{T, V\}$ , the margin  $\mathcal{M}_{u,m}$  measures the confidence with which the model distinguishes the positive target item embedding  $\mathbf{e}_{i^+}^m$  from a set of negative item embeddings  $\mathbf{e}_{i^-}^m$  ( $i^- \in \mathcal{N}_u$ ):

$$\mathcal{M}_{u,m} = s(\mathbf{z}_u^m, \mathbf{e}_{i^+}^m) - \frac{1}{|\mathcal{N}_u|} \sum_{i^- \in \mathcal{N}_u} s(\mathbf{z}_u^m, \mathbf{e}_{i^-}^m), \quad (6)$$

where  $s(\cdot, \cdot)$  denotes the cosine similarity. A larger  $\mathcal{M}_{u,m}$  implies stronger discriminative capability for that modality. Based on these margins, we dynamically identify the user-adaptive strong and weak modalities at each training step:

$$\mathcal{M}_{u,\text{strong}} = \max(\mathcal{M}_{u,T}, \mathcal{M}_{u,V}), \quad \mathcal{M}_{u,\text{weak}} = \min(\mathcal{M}_{u,T}, \mathcal{M}_{u,V}). \quad (7)$$

We then define the *Modality Gap*  $\Delta_{u,\text{gap}}$  as the disparity between these margins:

$$\Delta_{u,\text{gap}} = \text{sg}[\mathcal{M}_{u,\text{strong}}] - \mathcal{M}_{u,\text{weak}}, \quad (8)$$

where  $\text{sg}[\cdot]$  is the stop-gradient operator. By applying  $\text{sg}[\cdot]$  to  $\mathcal{M}_{u,\text{strong}}$ , it fixes the discriminative level of the strong modality as a *target lower bound*, ensuring that the model minimizes  $\Delta_{u,\text{gap}}$  by enhancing  $\mathcal{M}_{u,\text{weak}}$  rather than degrading  $\mathcal{M}_{u,\text{strong}}$ .

*Gap-guided Dynamic Penalty.* To explicitly reduce this gap, we convert  $\Delta_{u,\text{gap}}$  into a difficulty-aware penalty weight  $w_{u,\text{pen}}$ :

$$w_{u,\text{pen}} = 1 + \beta \cdot \text{Softplus}(\alpha \cdot \Delta_{u,\text{gap}}), \quad (9)$$

where  $\beta$  and  $\alpha$  are learnable parameters controlling the sensitivity of the penalty. As the discriminative gap increases for a specific user, meaning that the weak modality exhibits insufficient negative separation and thus  $\Delta_{u,\text{gap}}$  becomes larger,  $w_{u,\text{pen}}$  increases proportionally, and it converges to 1 as the two modalities become more balanced.

Finally,  $w_{u,\text{pen}}$  is integrated into the standard contrastive learning objective on the fused representation  $\mathbf{z}_u$ . Unlike conventional contrastive learning that treats all negatives uniformly,  $\mathcal{L}_{\text{WPCL}}$  amplifies the relative influence of negative samples via  $w_{u,\text{pen}}$ :

$$\mathcal{L}_{\text{WPCL}} = - \sum_{u \in \mathcal{B}} \log \frac{e^{s(\mathbf{z}_u, \mathbf{e}_{i^+}) / \tau_{\text{WPCL}}}}{e^{s(\mathbf{z}_u, \mathbf{e}_{i^+}) / \tau_{\text{WPCL}}} + w_{u,\text{pen}} \sum_{i^- \in \mathcal{N}_u} e^{s(\mathbf{z}_u, \mathbf{e}_{i^-}) / \tau_{\text{WPCL}}}} \quad (10)$$

where  $\tau_{\text{WPCL}}$  is the temperature of this objective. In this formulation, applying  $w_{u,\text{pen}} > 1$  to the negative term forces the model to perceive the negative samples as closer than they actually are. Since gradients flow through the fused representation  $\mathbf{z}_u = \mathbf{z}_u^T + \mathbf{z}_u^V$ , this amplified negative pressure serves a dual purpose: it maintains the

basic discriminative power of the strong modality while specifically concentrating gradient updates on the weak modality to satisfy the heightened separation requirement.

*4.2.2 Cross-modal Relational Topology Regularization.* While  $\mathcal{L}_{\text{WPCL}}$  effectively enforces negative separation in the weak modality, its aggressive pushing mechanism may cause the weak modality’s embedding space to undergo excessive expansion or distortion. This geometric misalignment disrupts semantic consistency across modalities, resulting in instability in the fusion process.

To mitigate this, we propose *Cross-modal Relational Topology Regularization* ( $\mathcal{L}_{\text{CRTR}}$ ). The core objective is not to enforce a strict point-wise alignment that makes embedding vectors identical. Such rigid metric learning can wash out modality-specific individualities by forcing one modality to simply relocate into the other’s embedding geometry. Instead, we focus on the relative similarity distributions between sequences and candidate items within each modality’s space, referred to as the *Relational Topology*, to ensure structural alignment across modalities. This approach preserves modality characteristics (e.g., linguistic nuances and visual patterns) while ensuring that semantic proximity in one modality translates to a consistent relative rank in the other.

Formally, for each modality  $m \in \{T, V\}$ , we perform *relational topology* alignment between the sequence representations and a candidate item representation set, denoted as  $C^m$ . In this work, we instantiate  $C^m$  using in-batch target items, i.e.,  $C^m = \{\mathbf{e}_j^m\}_{j=1}^B$ , for computational efficiency. We then compute the similarity matrix  $S_i^m \in \mathbb{R}^B$  between the  $i$ -th sequence  $\mathbf{z}_i^m$  and the  $j$ -th candidate item in  $C^m$  as follows:

$$S_{i,j}^m = s(\mathbf{z}_i^m, \mathbf{e}_j^m) / \tau_{\text{CRTR}}, \quad (11)$$

where  $\tau_{\text{CRTR}}$  is a temperature parameter.

We then apply a row-wise softmax to convert these similarities  $S_i^m$  into a probability distribution  $\mathbf{P}_i^m \in \mathbb{R}^B$ :

$$\mathbf{P}_{i,j}^m = \frac{\exp(S_{i,j}^m)}{\sum_{k=1}^B \exp(S_{i,k}^m)} \quad (12)$$

$\mathbf{P}_i^m$  reflects the relative similarity ranking structure in their representation space of how the  $i$ -th sequence ranks the candidate items relative to each other. We then align these relational topologies across modalities by minimizing the bidirectional Kullback-Leibler (KL) divergence between  $\mathbf{P}_i^T$  and  $\mathbf{P}_i^V$  of each  $i$ :

$$\mathcal{L}_{\text{CRTR}} = \frac{1}{2B} \sum_{i=1}^B \left( \text{KL}(\mathbf{P}_i^T \parallel \mathbf{P}_i^V) + \text{KL}(\mathbf{P}_i^V \parallel \mathbf{P}_i^T) \right) \quad (13)$$

Consequently,  $\mathcal{L}_{\text{CRTR}}$  guides the weak modality to maintain a consistent semantic neighborhood structure with the strong modality. This effectively suppresses the geometric distortion that may arise from the aggressive negative pushing of  $\mathcal{L}_{\text{WPCL}}$ , stabilizing the multimodal fusion.

*4.2.3 Final Objective.* Finally, we combine the proposed loss functions to optimize the model jointly. The total objective function  $\mathcal{L}$  is defined as follows:

$$\mathcal{L} = \mathcal{L}_{\text{WPCL}} + \lambda \cdot \mathcal{L}_{\text{CRTR}} \quad (14)$$

where  $\lambda$  is a hyperparameter that balances discrimination and structural consistency. This synergy balances  $\mathcal{L}_{\text{WPCL}}$ ’s discriminative

**Table 2: Performance comparison on Task 1 across various methods. The best results are highlighted in bold, second-best results are underlined, and \* denotes statistical significance with p-values < 0.05, based on paired t-tests over 5 random seeds.**

Method	Toys				Beauty				Clothing				Sports			
	H@10	H@20	N@10	N@20												
<b>ID-based Models</b>																
GRU4Rec	0.3591	0.4596	0.2295	0.2548	0.3903	0.4898	0.2624	0.2875	0.3450	0.4781	0.2025	0.2360	0.3500	0.4558	0.2165	0.2431
SASRec	0.3812	0.4780	0.2613	0.2856	0.4280	0.5283	0.2984	0.3236	0.3442	0.4757	0.2097	0.2428	0.3834	0.4935	0.2448	0.2726
<b>Text-based Models</b>																
BERT	0.1242	0.2336	0.0579	0.0853	0.1372	0.2602	0.0671	0.0978	0.1294	0.2558	0.0586	0.0904	0.1239	0.2379	0.0572	0.0857
SLIM	0.1217	0.2474	0.0567	0.0880	0.1412	0.2724	0.0661	0.0987	0.1374	0.2747	0.0632	0.0975	0.1254	0.2510	0.0575	0.0889
SLIM <sup>+</sup>	0.2839	0.4208	0.1625	0.1968	0.2715	0.4112	0.1504	0.1854	0.1801	0.3686	0.0820	0.1291	0.1619	0.3148	0.0776	0.1157
LLMEMB	0.3944	0.5278	0.2447	0.2783	0.3109	0.5836	0.2388	0.2810	0.3987	0.5490	0.2317	0.2696	0.4046	0.5882	0.2228	0.2692
LLM2Rec	0.3172	0.4718	0.1875	0.2262	0.3282	0.4769	0.1854	0.2227	0.3264	0.4676	0.1829	0.2184	0.3600	0.5421	0.1915	0.2374
LLM <sub>vanilla</sub>	0.2419	0.3597	0.1452	0.1747	0.2300	0.3428	0.1353	0.1636	0.2849	0.4052	0.1663	0.1966	0.2225	0.3471	0.1264	0.1577
LLM <sub>SFT</sub>	<u>0.4287</u>	0.5669	<u>0.2712</u>	<u>0.3061</u>	<u>0.4963</u>	0.6347	<u>0.3085</u>	0.3434	0.4333	0.6049	0.2525	0.2957	<u>0.4863</u>	<u>0.6684</u>	<u>0.2797</u>	<u>0.3265</u>
<b>Multimodal-based Models</b>																
CLIP	0.3258	0.4342	0.2069	0.2341	0.2114	0.2819	0.1318	0.1494	0.3061	0.4043	0.1887	0.2135	0.2630	0.3698	0.1495	0.1764
NoteLLM-2	0.2237	0.4545	0.1003	0.1582	0.1926	0.3536	0.0929	0.1331	0.1764	0.3431	0.0815	0.1233	0.1993	0.3884	0.0932	0.1440
VLM <sub>prompt</sub>	0.2892	0.4205	0.1717	0.2046	0.2193	0.3367	0.1190	0.1485	0.2578	0.3829	0.1485	0.1799	0.2355	0.3588	0.1301	0.1610
VLM <sub>vanilla</sub> (Int.)	0.3184	0.4245	0.2093	0.2360	0.2146	0.2986	0.1358	0.1569	0.2661	0.3577	0.1830	0.2060	0.3045	0.3840	0.2113	0.2313
VLM <sub>vanilla</sub> (Ext.)	0.2659	0.4222	0.1426	0.1817	0.2096	0.3379	0.1097	0.1419	0.2459	0.3799	0.1375	0.1711	0.2538	0.3803	0.1203	0.1761
VLM <sub>SFT</sub> (Int.)	0.3381	0.5131	0.1770	0.2209	0.4100	0.5794	0.2941	<u>0.3498</u>	0.4531	0.6178	0.3015	0.3284	0.4588	0.6383	0.2720	0.3093
VLM <sub>SFT</sub> (Ext.)	0.4160	<u>0.5897</u>	0.2209	0.2647	0.4038	<u>0.6372</u>	0.2744	0.3300	<u>0.5022</u>	<u>0.6474</u>	<u>0.3164</u>	<u>0.3531</u>	0.4795	0.6291	0.2783	0.3161
VLM2Rec	<b>0.5225*</b>	<b>0.6476*</b>	<b>0.3578*</b>	<b>0.3893*</b>	<b>0.5644*</b>	<b>0.6822*</b>	<b>0.3824*</b>	<b>0.4121*</b>	<b>0.5627*</b>	<b>0.7182*</b>	<b>0.3458*</b>	<b>0.3851*</b>	<b>0.5574*</b>	<b>0.6993*</b>	<b>0.3694*</b>	<b>0.4052*</b>
Improv. (%)	21.88	9.82	31.93	27.18	13.72	7.06	23.95	17.81	12.05	10.94	9.29	9.06	14.62	4.62	32.07	24.10

**Table 3: Statistics of datasets used in the experiments.**

Dataset	#Users	#Items	#Interactions	Avg. Length	Sparsity (%)
Toys	15,921	8,383	108,336	6.8	99.92
Beauty	19,757	9,311	137,300	6.9	99.93
Clothing	30,757	17,087	196,614	6.4	99.96
Sports	32,127	14,820	222,591	6.9	99.95

push with  $\mathcal{L}_{\text{CRTR}}$ 's structural alignment to ensure a stable and robust multimodal space.

## 5 Experiments

### 5.1 Experimental Setup

**5.1.1 Implementation Details.** We utilize four Amazon<sup>1</sup> domains [24] (Toys, Beauty, Clothing, Sports) with 5-core filtering [14], excluding items missing titles or images. Statistics of datasets are reported in Tab. 3. Following [8], we set the max sequence length to 10 and use leave-one-out protocol [14, 31, 47]. Hyperparameters are tuned via grid search:  $\tau_{\text{WPCL}} \in \{0.05, 0.1, 0.5, 1.0\}$ ,  $\tau_{\text{CRTR}} \in \{0.001, 0.01, 0.1, 1.0\}$ , and  $\lambda \in \{0.1, 0.5, 1.0\}$ . We employ LoRA [11] ( $\text{rank}=16$ ,  $\alpha=32$ ,  $\text{dropout}=0.2$ ) on Qwen2.5-VL-3B [3] (Qwen2.5-3B [29] for LLM), which also serves as the backbone for all baselines to ensure fairness. Training runs for 3 epochs using AdamW [23] (learning rate  $1e-5$ , batch size 8), gradient checkpointing on a single RTX 3090. For some experiments that require full-parameter tuning or large models, we train on a single A100 80GB. Other settings follow their own paper.

<sup>1</sup><https://jmcauley.ucsd.edu/data/amazon/>

**5.1.2 Baselines.** To demonstrate the effectiveness of VLM2Rec, we compare it against baselines across five categories: (1) **ID-based SR models**, including RNN-based GRU4Rec [9] and transformer-based SASRec [14]; (2) **Small pretrained encoders** utilizing BERT<sup>2</sup> [6] for text and CLIP<sup>3</sup> [30] for multimodal settings; (3) **Large foundation models** in both vanilla (LLM<sub>vanilla</sub>, VLM<sub>vanilla</sub>) and SFT variants (LLM<sub>SFT</sub>, VLM<sub>SFT</sub>); (4) **Recommendation-specific embedders** comprising LLM-based frameworks (LLMEmb [21], LLM2Rec [8], SLIM [41], SLIM<sup>+</sup>) and VLM-based embedders (VLM<sub>prompt</sub> [27], NoteLLM-2 [44]); and (5) standard **Fusion strategies** between Internal (Int.) and External (Ext.) fusion to validate our encoding approach.

**5.1.3 Evaluation Settings.** For all experiments, we use 100 negative samples and report Hit Rate (H@K) and Normalized Discounted Cumulative Gain (N@K) at  $K \in \{10, 20\}$ , averaged over 5 random seeds. As shown in Fig. 2 (left), we evaluate embedding quality via two real-world tasks:

**Task 1) Direct Recommendation.** Adopting the standard retrieval setting, we rank items based on vector similarity to verify the capture of CF signals while retaining rich semantics (Tab. 2). To enable comparison for only producing item embeddings, we derive sequence representations by mean-pooling historical item embeddings.

**Task 2) Downstream SR Model Initialization.** We test whether the embeddings provide transferable initialization for standard SR

<sup>2</sup>google-bert/bert-large-uncased

<sup>3</sup>openai/clip-vit-large-patch14

**Table 4: Performance comparison on Task 2 across various methods. The best results are highlighted in bold, second-best results are underlined, and \* denotes statistical significance with p-values < 0.05, based on paired t-tests over 5 random seeds.**

Method	Toys				Beauty				Clothing				Sports			
	H@10	H@20	N@10	N@20												
<b>Backbone: GRU4Rec</b>																
GRU4Rec	0.3591	0.4596	0.2295	0.2548	0.3903	0.4898	0.2624	0.2875	0.3450	0.4781	0.2025	0.2360	0.3500	0.4558	0.2165	0.2431
<b>Text-based Models</b>																
BERT	0.3320	0.4419	0.1890	0.2248	0.3704	0.4847	0.2349	0.2637	0.3325	0.4759	0.1875	0.2236	0.3402	0.4707	0.1995	0.2325
SLIM	0.3456	0.4606	0.2146	0.2435	0.3728	0.4929	0.2500	0.2732	0.3265	0.4677	0.1842	0.2196	0.4209	0.5473	0.2612	0.2931
SLIM*	0.4105	0.5259	0.2632	0.2923	0.4383	0.5465	0.2933	0.3204	0.3761	0.5141	0.2222	0.2570	0.4507	0.5847	0.2794	0.3132
LLMEmb	0.4316	0.5405	0.2755	0.3033	0.4593	0.5583	0.2957	0.3286	0.3929	0.5264	0.2397	0.2748	0.4608	0.5892	0.2917	0.3209
LLM2Rec	0.4107	0.5261	0.2634	0.2926	0.4396	0.5480	0.2938	0.3212	0.3820	0.5261	0.2263	0.2625	0.4480	0.5831	0.2786	0.3127
LLM <sub>Vanilla</sub>	0.3759	0.4943	0.2310	0.2609	0.4215	0.5384	0.2728	0.3023	0.3684	0.5025	0.2165	0.2500	0.4260	0.5703	0.2523	0.2887
LLM <sub>SFT</sub>	<u>0.4381</u>	<u>0.5568</u>	0.2757	0.3082	<u>0.4603</u>	<u>0.5690</u>	0.2979	0.3253	0.4092	<u>0.5485</u>	0.2467	0.2825	<u>0.4687</u>	0.6026	0.2934	<u>0.3273</u>
<b>Multimodal-based Models</b>																
CLIP	0.3684	0.4646	0.2125	0.2339	0.4324	0.5378	0.2862	0.3127	0.3561	0.4684	0.2193	0.2476	0.3796	0.4950	0.2305	0.2597
NoteLLM-2	0.4187	0.5436	0.2656	0.2909	0.4557	0.5588	<u>0.3028</u>	0.3266	0.4006	0.5256	0.2351	0.2685	0.4638	0.5934	0.2804	0.3090
VLM <sub>Prompt</sub>	0.3890	0.5002	0.2465	0.2746	0.4252	0.5415	0.2752	0.3044	0.3791	0.5135	0.2269	0.2607	0.4297	0.5731	0.2558	0.2920
VLM <sub>Vanilla</sub> (Int.)	0.4000	0.5105	0.2557	0.2836	0.4376	0.5485	0.2933	0.3212	0.3640	0.5040	0.2144	0.2498	0.4456	0.5806	0.2764	0.3105
VLM <sub>Vanilla</sub> (Ext.)	0.3983	0.5099	0.2565	0.2844	0.4358	0.5427	0.2882	0.3094	0.3698	0.5081	0.2185	0.2533	0.4432	0.5768	0.2746	0.3083
VLM <sub>SFT</sub> (Int.)	0.4204	0.5399	0.2743	0.3005	0.4393	0.5383	0.2930	0.3151	0.4093	0.5339	0.2413	0.2741	0.4594	0.6003	0.2869	0.3219
VLM <sub>SFT</sub> (Ext.)	0.4363	0.5505	<u>0.2834</u>	<u>0.3122</u>	0.4511	0.5604	0.3021	<u>0.3296</u>	<u>0.4130</u>	0.5432	<u>0.2527</u>	<u>0.2856</u>	0.4662	<u>0.6193</u>	<u>0.2945</u>	0.3254
<b>VLM2Rec</b>	<b>0.4684*</b>	<b>0.5869*</b>	<b>0.3070*</b>	<b>0.3369*</b>	<b>0.5064*</b>	<b>0.6185*</b>	<b>0.3386*</b>	<b>0.3669*</b>	<b>0.4405*</b>	<b>0.5778*</b>	<b>0.2711*</b>	<b>0.3057*</b>	<b>0.5021*</b>	<b>0.6468*</b>	<b>0.3083*</b>	<b>0.3449*</b>
Improv. (%)	6.92	5.41	8.21	7.91	10.02	8.71	11.82	11.32	6.66	5.34	7.28	7.04	7.13	4.44	4.69	5.38
<b>Backbone: SASRec</b>																
SASRec	0.3812	0.4780	0.2613	0.2856	0.4280	0.5283	0.2984	0.3236	0.3442	0.4757	0.2097	0.2428	0.3834	0.4935	0.2448	0.2726
<b>Text-based Models</b>																
BERT	0.3549	0.4752	0.2347	0.2450	0.3608	0.4767	0.2319	0.2611	0.3111	0.4495	0.1793	0.2141	0.3409	0.4544	0.2019	0.2371
SLIM	0.3570	0.4765	0.2302	0.2602	0.3546	0.4723	0.2269	0.2566	0.3034	0.4343	0.1773	0.2102	0.3803	0.4909	0.2423	0.2702
SLIM*	0.4486	0.5626	0.3078	0.3365	0.4683	0.5748	0.3255	0.3523	0.3566	0.4859	0.2145	0.2470	0.4680	0.6012	0.2988	0.3324
LLMEmb	0.4441	0.5570	0.3047	0.3331	0.4735	0.5888	0.3267	0.3566	0.3822	0.5262	0.2422	0.2748	0.4911	0.6260	0.3096	0.3454
LLM2Rec	0.4362	0.5468	0.2995	0.3273	0.4657	0.5726	0.3244	0.3513	0.3732	0.5128	0.2245	0.2596	0.4735	0.6106	0.3013	0.3359
LLM <sub>Vanilla</sub>	0.4374	0.5564	0.2912	0.3212	0.4440	0.5604	0.2932	0.3226	0.3793	0.5153	0.2276	0.2620	0.4284	0.5728	0.2579	0.2944
LLM <sub>SFT</sub>	<u>0.4636</u>	<u>0.5735</u>	0.3066	<u>0.3386</u>	<u>0.4956</u>	<u>0.5912</u>	0.3266	0.3553	0.4245	<u>0.5698</u>	0.2554	0.2920	<u>0.4924</u>	<u>0.6321</u>	0.3116	<u>0.3470</u>
<b>Multimodal-based Models</b>																
CLIP	0.3745	0.4672	0.2570	0.2804	0.3846	0.4733	0.2618	0.2842	0.3328	0.4884	0.2374	0.2662	0.3833	0.4991	0.2366	0.2659
NoteLLM-2	0.4601	0.5637	0.2938	0.3365	0.4755	0.5843	0.3217	0.3507	0.4073	0.5347	0.2577	0.2547	0.4803	0.6055	0.2983	0.3163
VLM <sub>Prompt</sub>	0.4440	0.5605	0.2976	0.3268	0.4475	0.5614	0.2980	0.3267	0.3862	0.5228	0.2368	0.2713	0.4455	0.5936	0.2700	0.3074
VLM <sub>Vanilla</sub> (Int.)	0.4444	0.5560	0.3033	0.3314	0.4597	0.5655	0.3191	0.3457	0.3830	0.5066	0.2455	0.2847	0.4332	0.5593	0.2764	0.3082
VLM <sub>Vanilla</sub> (Ext.)	0.4469	0.5562	0.3015	0.3322	0.4535	0.5605	0.3141	0.3408	0.3819	0.5236	0.2307	0.2663	0.4426	0.5702	0.2826	0.3148
VLM <sub>SFT</sub> (Int.)	0.4557	0.5526	<u>0.3099</u>	0.3325	0.4783	0.5832	0.3214	0.3468	0.4296	0.5394	0.2593	0.3003	0.4823	0.6055	0.3023	0.3204
VLM <sub>SFT</sub> (Ext.)	0.4605	0.5718	0.3081	0.3356	0.4805	0.5890	<u>0.3298</u>	<u>0.3570</u>	<u>0.4334</u>	0.5647	<u>0.2704</u>	<u>0.3036</u>	0.4883	0.6153	<u>0.3120</u>	0.3441
<b>VLM2Rec</b>	<b>0.4889*</b>	<b>0.6074*</b>	<b>0.3340*</b>	<b>0.3639*</b>	<b>0.5346*</b>	<b>0.6466*</b>	<b>0.3649*</b>	<b>0.3932*</b>	<b>0.4585*</b>	<b>0.6004*</b>	<b>0.2899*</b>	<b>0.3257*</b>	<b>0.5273*</b>	<b>0.6737*</b>	<b>0.3287*</b>	<b>0.3657*</b>
Improv. (%)	5.46	5.91	7.78	7.47	7.87	9.37	10.64	10.14	5.79	5.37	7.21	7.28	7.09	6.58	5.35	5.39

backbones, shown in Tab. 4 (e.g., GRU4Rec [9], SASRec [14]). Dimensions are matched via a 1-layer linear adapter to the backbone hidden size ( $d=128$ ). And we follow the adaptation methods if described in their original paper.

## 5.2 Task 1: Direct Recommendation

**Text vs. Multimodal Signals.** Even with small encoders, visual signals are beneficial (CLIP > BERT), and VLM-based embeddings outperform LLM-only embeddings in the vanilla setting, suggesting complementary visual cues.

**Capacity and CF Injection.** While large foundation models outperform small encoders, vanilla variants still lag behind ID-based

SR, indicating that semantics alone are insufficient. SFT models surpass ID baselines, confirming that injecting CF signals in item embeddings is essential.

**Importance of Sequence-level SFT.** SFT models consistently outperform recommendation specific SOTA models. The latter lacks explicit sequence-level representation space optimization, failing to capture transition signals essential for SR task.

**Modality Paradox.** Despite  $VLM_{Vanilla} > LLM_{Vanilla}$ ,  $VLM_{SFT}$  often lags behind  $LLM_{SFT}$ . This confirms our analysis: SFT induces modality collapse, causing under-optimized visual embeddings to act as negative transfer.

**Table 5: We analyze the detailed mechanisms for the ablation study and the fusion strategies in Task 1, 2 (SASRec) on Beauty and Toys. (N@20)**

Variants	Beauty		Toys	
	Task 1	Task 2	Task 1	Task 2
	<b>VLM2Rec (Ours)</b>	<b>0.4121</b>	<b>0.3932</b>	<b>0.3893</b>
w/o $\mathcal{L}_{WPCL}$	0.2592	0.3605	0.2318	0.3486
→ w/ $\mathcal{L}_{WPCL}$ w/o Stop Grad.	0.4031	0.3774	0.3806	0.3514
→ w/ $\mathcal{L}_{WPCL}$ w/o $w_{pen}$	0.3985	0.3709	0.3712	0.3472
w/o $\mathcal{L}_{CRTR}$	0.4058	0.3785	0.3802	0.3515

**Fusion Strategy Reversal.** While internal fusion favors vanilla models, external fusion becomes superior post-SFT, suggesting it effectively mitigates cross-modal interference during optimization.

### 5.3 Task 2: Downstream SR Model Initialization

**Correlation with Task 1.** Performance trends in Task 2 follow Task 1, confirming that initialization enriched with rich semantics and CF signals provides a superior optimization starting point, allowing backbones to focus on refining complex patterns.

**Comparison with Rec-trained Models.** While fine-tuned baselines incorporate CF signals, they remain suboptimal for SR initialization due to structural limitations. LLMemb relies on indirect distillation, whereas generative models (SLIM<sup>+</sup>, LLM2Rec) optimize next token probabilities rather than representation space geometry. Furthermore, item-centric approaches (LLM2Rec, NoteLLM-2) fail to encode sequence transition dynamics, resulting in poor alignment with downstream sequential tasks.

**Backbone-agnostic Robustness.** VLM2Rec shows the most consistent performance gains across both the RNN-based GRU4Rec and the Transformer-based SASRec backbones. This demonstrates that it captures general sequence dynamics independent of backbone-specific inductive biases, serving as a robust, plug-and-play initializer.

### 5.4 Further Analysis

**5.4.1 Ablation Study.** Table 5 validates the efficacy of each component. Removing  $\mathcal{L}_{WPCL}$  causes the sharpest drop, confirming its fundamental role in injecting CF signals and adapting the VLM for retrieval. The performance gain from  $w_{pen}$  over standard SFT proves that penalizing the weak modality effectively mitigates shortcut learning. The stop-gradient is crucial; without it, the model minimizes the modality gap by degrading the strong modality rather than improving the weak one. Furthermore,  $\mathcal{L}_{CRTR}$  acts as a necessary regularizer, maintaining geometric consistency against the aggressive negative pushing of  $\mathcal{L}_{WPCL}$ .

**5.4.2 Analysis of Resolving Modality Collapse.** As shown in Fig. 1b, VLM2Rec substantially mitigates the rapid drop in weak-modality gradient contribution observed during standard SFT. This is driven by  $\mathcal{L}_{WPCL}$ , which increases penalties on weak-modality negatives to restore discriminative learning, and  $\mathcal{L}_{CRTR}$ , which stabilizes cross-modal geometry. Table 1 confirms that VLM2Rec fully recovers the geometric collapse in the image space (previously  $S \leq 1$  with

**Table 6: Performance comparison on Cross-Domain Recommendation across Task 1, 2 (N@20).**

Model	Clothing → Beauty		Sports → Clothing	
	Task 1	Task 2	Task 1	Task 2
LLMEMB	0.2676	0.3408	0.2589	0.2667
LLM <sub>SFT</sub>	0.1899	0.3326	0.1179	0.2600
NoteLLM-2	0.1185	0.3237	0.0747	0.2988
VLM <sub>SFT</sub>	0.2566	0.3449	0.2362	0.2955
<b>VLM2Rec</b>	<b>0.3372</b>	<b>0.3840</b>	<b>0.3154</b>	<b>0.3214</b>

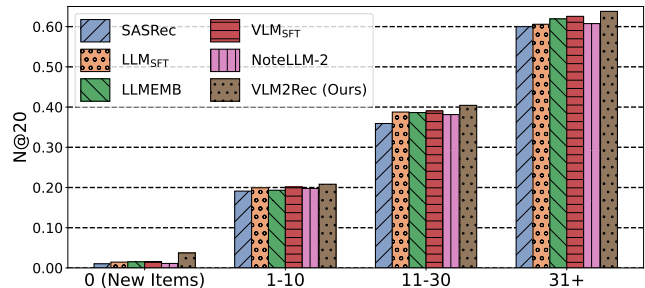


**Figure 3: Cold-start evaluation on the Beauty for Task 2 (SASRec), grouped by target item frequency in the training set.**

degraded  $U$ ): all modalities achieve  $S > 1$  with improved uniformity  $U$ , indicating clear positive–negative separation and better space utilization. Moreover, while the fused space previously mirrored the text space, VLM2Rec increases the effective contribution of the image modality. As a result, Fig. 1a shows a marked improvement in  $v2f$ , and multimodal fusion becomes synergistic rather than harmful, with  $f2f$  consistently outperforming  $t2f$  and  $v2f$  across datasets. On Beauty, in particular, VLM2Rec slightly reduces over-reliance on text while substantially strengthening visual utilization, yielding the best fused performance. Overall, these results show that VLM2Rec converts multimodal signals into recommendation gains by balancing modality gradients and preventing representation collapse.

**5.4.3 Generalization Analysis via Rich Semantics.** We examine generalization when CF signals are scarce or unreliable via two settings: *cross-domain transfer* (Tab. 6) and *cold-start items* (Fig. 3). In both cases, effective recommendation depends more on rich modality semantics and sequence reasoning than memorized co-occurrence. For *cross-domain transfer*, we perform zero-shot evaluation by training on a source domain and directly testing on a target domain, where domain shift makes CF regularities less reliable. VLM2Rec achieves the best results across both transfers and both tasks, indicating that its balanced multimodal representations capture more transferable preference patterns and avoid domain-specific overfitting. For *cold-start items*, we bucket target items by training frequency and evaluate Task 2. As frequency decreases, performance increasingly reflects semantic exploitation rather than CF memorization. VLM2Rec effectively synergizes deep item understanding with sequence reasoning to infer preferences solely from attributes. These results demonstrate that balanced multimodal semantics and

**Table 7: Performance and Efficiency comparison for Task 1,2.  $K$  is the # of sampled users in the train dataset. Times are reported in minutes per epoch and seconds for item embedding generation ( $N@20$ ).**

Model	Input	Task 1	Task 2	Train (min)	Emb. (sec)
<b>Beauty</b>					
LLMEMB	Item	0.2810	0.3566	22	58
LLM2Rec	Seq./Item	0.2227	0.3513	33	58
LLM <sub>SFT</sub>	Seq.	0.3434	0.3553	35	56
NoteLLM-2	Item	0.1331	0.3507	26	132
VLM <sub>SFT</sub>	Seq.	0.3300	0.3570	117	113
VLM2Rec ( $K=128$ )		0.2038	0.3635	1	
VLM2Rec ( $K=256$ )		0.2377	0.3633	2	
VLM2Rec ( $K=512$ )	Seq.	0.2816	0.3648	4	113
VLM2Rec ( $K=1024$ )		0.3345	0.3678	9	
VLM2Rec (Full)		0.4121	0.3932	118	
<b>Toys</b>					
LLMEMB	Item	0.2783	0.3331	15	38
LLM2Rec	Seq./Item	0.2262	0.3273	26	39
LLM <sub>SFT</sub>	Seq.	0.3061	0.3386	26	39
NoteLLM-2	Item	0.1582	0.3365	20	91
VLM <sub>SFT</sub>	Seq.	0.2647	0.3356	92	79
VLM2Rec ( $K=128$ )		0.2278	0.3430	1	
VLM2Rec ( $K=256$ )		0.2490	0.3426	2	
VLM2Rec ( $K=512$ )	Seq.	0.2997	0.3451	4	79
VLM2Rec ( $K=1024$ )		0.3266	0.3475	7	
VLM2Rec (Full)		0.3893	0.3639	95	

sequence-aware alignment enable robust recommendations even when historical interactions are weak or absent.

**5.4.4 Analysis of Model Scalability and Robustness.** To verify generalizability, we evaluated various VLM families (e.g., Qwen2.5-VL [3], InternVL3 [49], Llava 1.5 [20]) with parameter sizes ranging from 2B to 32B, shown in Fig. 4. Models within similar parameter groups (e.g., 2–3B, 7–8B) demonstrated comparable performance, indicating robustness across different architectures. Overall, performance improves with capacity by leveraging richer prior knowledge, suggesting that parameter size can be chosen according to deployment objectives.

**5.4.5 Computational Cost and Few-shot Efficiency.** Tab. 7 reports training time and item embedding generation time across LLM/VLM methods. While VLM-based models (VLM<sub>SFT</sub>, VLM2Rec) incur higher costs due to image token processing compared to text-only LLMs, the runtime similarity between VLM2Rec and VLM<sub>SFT</sub> confirms that our objectives introduce little overhead. To mitigate training costs, we train VLM2Rec with only  $K$  randomly sampled users: even at  $K=128$  it outperforms some full-training baselines and surpasses most methods on Task 2, and at  $K=1024$  (about 5–6% of training data) it matches the strongest baseline while substantially reducing training time. Consequently, our framework provides a tunable trade-off, allowing practitioners to substantially reduce training time while maintaining competitive performance under varying constraints.

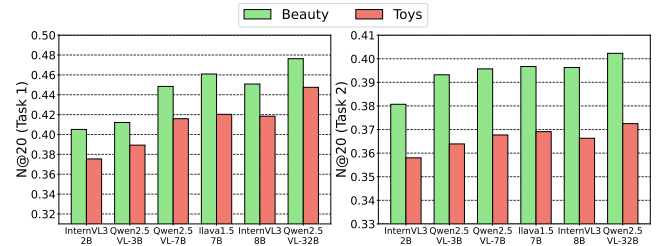


**Figure 4: Performance of VLM2Rec across various VLM families and parameter sizes, reporting  $N@20$  for Task 1 and Task 2.**

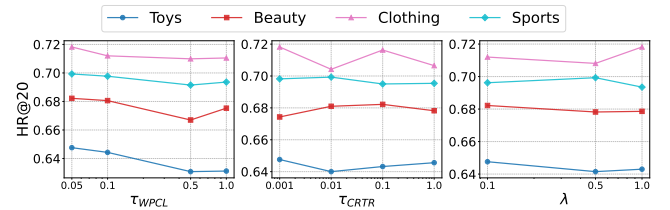


**Figure 5: Impact of hyperparameters  $\tau_{WPCL}$ ,  $\tau_{CRTR}$ , and  $\lambda$ .**

**5.4.6 Hyperparameter Sensitivity.** We conduct a sensitivity analysis of VLM2Rec by varying hyperparameters across the search space. In Fig. 5, VLM2Rec consistently maintains superior performance over baselines with minimal variance across varying hyperparameter values, demonstrating its robust stability. This reduces the additional tuning cost often required by multi-objective training, making VLM2Rec a practical and stable solution across diverse domains.

## 6 Related Works

**Multimodal Sequential Recommendation** While early fusion strategies [5, 12, 43] and modern architectures [4, 10, 37] incorporate side information, they typically rely on *frozen* encoders. Unlike ID-based models [9, 14], where learnable tables absorb collaborative signals, frozen encoders shift the learning burden to the backbone. This necessitates a shift toward CF-aware modality embeddings that enable direct ranking without ID dependence.

**Large Model Embedders for Multimodal Recommendation** Recent NLP work repurposes LLMs as high-capacity encoders for representation learning [16–18, 36, 38]. Following this trend, SLIM [41] distills sequence knowledge from ChatGPT [1], LLMemb [21] learns discriminative item embeddings and injects CF signals via pre-trained ID embedding guidance, and LLM2Rec [8] injects CF through generative next-item prediction and item-level contrastive stage. In multimodal settings, VLM<sub>prompt</sub> [27] leverages zero-shot prompting, and NoteLLM-2 [44] focuses on enhancing visual representation in multimodal embedding. However, these methods largely emphasize item-level discrimination or inject sequence-level CF indirectly (often via generative objectives), which does not explicitly shape a sequence–item representation space for SR. Our

work encodes image sequences alongside text using VLM multi-image reasoning [3, 20, 49], explicitly internalizing sequence-level CF signals into a multimodal embedding space.

**Modality Collapse in Multimodal Learning** Multimodal models often over-rely on an easier modality, under-utilizing the others. Prior studies analyze how dataset/model biases induce imbalanced optimization and propose mitigation strategies [7, 13, 34, 40, 42], while related work shows VLM embeddings can become organized around a dominant modality [19, 33, 46]. We empirically establish that this persists in SR and is amplified by standard contrastive SFT despite its necessity for CF injection. Accordingly, our framework explicitly enforces balanced modality utilization to stabilize the learned representation geometry.

## 7 Conclusion

In this work, we propose VLM2Rec, a novel framework that leverages VLMs as embedders for multimodal sequential recommendation, encoding both visual and textual sequences to inject sequence-level collaborative filtering signals. Our analysis revealed that the intrinsic modality bias of VLMs leads to representation collapse, a critical issue exacerbated by standard fine-tuning that hinders recommendation accuracy. To address this issue, VLM2Rec dynamically identifies the weak modality during training and explicitly improves its discriminability while preserving cross-modal consistency. Extensive experiments on public benchmarks demonstrate that our method consistently improves both direct ranking and downstream SR initialization across model families and settings.

## References

- [1] Josh Achiam, Steven Adler, Sandhini Agarwal, Lama Ahmad, Ilge Akkaya, Florencia Leoni Aleman, Diogo Almeida, Janko Altschmidt, Sam Altman, Shyamal Anadkat, et al. 2023. Gpt-4 technical report. *arXiv preprint arXiv:2303.08774* (2023).
- [2] Devansh Arpit, Stanislaw Jastrzyski, Nicolas Ballas, David Krueger, Emmanuel Bengio, Maxinder S Kanwal, Tegan Maharaj, Asja Fischer, Aaron Courville, Yoshua Bengio, et al. 2017. A closer look at memorization in deep networks. In *International conference on machine learning*. PMLR, 233–242.
- [3] Shuai Bai, Keqin Chen, Xuejing Liu, Jialin Wang, Wenbin Ge, Sibao Song, Kai Dang, Peng Wang, Shijie Wang, Jun Tang, et al. 2025. Qwen2.5-vl technical report. *arXiv preprint arXiv:2502.13923* (2025).
- [4] Shuqing Bian, Xingyu Pan, Wayne Xin Zhao, Jinpeng Wang, Chuyuan Wang, and Ji-Rong Wen. 2023. Multi-modal mixture of experts representation learning for sequential recommendation. In *Proceedings of the 32nd ACM international conference on information and knowledge management*. 110–119.
- [5] Qiang Cui, Shu Wu, Qiang Liu, Wen Zhong, and Liang Wang. 2018. MV-RNN: A multi-view recurrent neural network for sequential recommendation. *IEEE Transactions on Knowledge and Data Engineering* 32, 2 (2018), 317–331.
- [6] Jacob Devlin, Ming-Wei Chang, Kenton Lee, and Kristina Toutanova. 2019. Bert: Pre-training of deep bidirectional transformers for language understanding. In *Proceedings of the 2019 conference of the North American chapter of the association for computational linguistics: human language technologies, volume 1 (long and short papers)*. 4171–4186.
- [7] Yangyang Guo, Liqiang Nie, Harry Cheng, Zhiyong Cheng, Mohan Kankanhalli, and Alberto Del Bimbo. 2023. On modality bias recognition and reduction. *ACM Transactions on Multimedia Computing, Communications and Applications* 19, 3 (2023), 1–22.
- [8] Yingzhi He, Xiaohao Liu, An Zhang, Yunshan Ma, and Tat-Seng Chua. 2025. LLM2Rec: Large Language Models Are Powerful Embedding Models for Sequential Recommendation. In *Proceedings of the 31st ACM SIGKDD Conference on Knowledge Discovery and Data Mining V.2 (Toronto ON, Canada) (KDD '25)*. Association for Computing Machinery, New York, NY, USA, 896–907. doi:10.1145/3711896.3737029
- [9] Balázs Hidasi, Alexandros Karatzoglou, Linas Baltrunas, and Domonkos Tikk. 2015. Session-based recommendations with recurrent neural networks. *arXiv preprint arXiv:1511.06939* (2015).
- [10] Yupeng Hou, Shanlei Mu, Wayne Xin Zhao, Yaliang Li, Bolin Ding, and Ji-Rong Wen. 2022. Towards universal sequence representation learning for recommender systems. In *Proceedings of the 28th ACM SIGKDD conference on knowledge discovery and data mining*. 585–593.
- [11] Edward J Hu, Yelong Shen, Phillip Wallis, Zeyuan Allen-Zhu, Yuanzhi Li, Shean Wang, Lu Wang, Weizhu Chen, et al. 2022. Lora: Low-rank adaptation of large language models. *ICLR* 1, 2 (2022), 3.
- [12] Hengchang Hu, Wei Guo, Yong Liu, and Min-Yen Kan. 2023. Adaptive multi-modalities fusion in sequential recommendation systems. In *Proceedings of the 32nd ACM International Conference on Information and Knowledge Management*. 843–853.
- [13] Yu Huang, Junyang Lin, Chang Zhou, Hongxia Yang, and Longbo Huang. 2022. Modality competition: What makes joint training of multi-modal network fail in deep learning?(provably). In *International conference on machine learning*. PMLR, 9226–9259.
- [14] Wang-Cheng Kang and Julian McAuley. 2018. Self-attentive sequential recommendation. In *2018 IEEE international conference on data mining (ICDM)*. IEEE, 197–206.
- [15] JuneHyoun Kwon, MiHyeon Kim, Eunju Lee, Juhwan Choi, and YoungBin Kim. 2025. See-Saw Modality Balance: See Gradient, and Sew Impaired Vision-Language Balance to Mitigate Dominant Modality Bias. *arXiv preprint arXiv:2503.13834* (2025).
- [16] Chankyu Lee, Rajarshi Roy, Mengyao Xu, Jonathan Raiman, Mohammad Shoeybi, Bryan Catanzaro, and Wei Ping. 2024. Nv-embed: Improved techniques for training llms as generalist embedding models. *arXiv preprint arXiv:2405.17428* (2024).
- [17] Chaofan Li, Minghao Qin, Shitao Xiao, Jianyu Chen, Kun Luo, Yingxia Shao, Defu Lian, and Zheng Liu. 2024. Making text embedders few-shot learners. *arXiv preprint arXiv:2409.15700* (2024).
- [18] Shiyu Li, Yang Tang, Ruijie Liu, Shi-Zhe Chen, and Xi Chen. 2025. Conan-embedding-v2: Training an llm from scratch for text embeddings. In *Proceedings of the 2025 Conference on Empirical Methods in Natural Language Processing*. 15011–15027.
- [19] Victor Weixin Liang, Yuhui Zhang, Yongchan Kwon, Serena Yeung, and James Y Zou. 2022. Mind the gap: Understanding the modality gap in multi-modal contrastive representation learning. *Advances in Neural Information Processing Systems* 35 (2022), 17612–17625.
- [20] Haotian Liu, Chunyuan Li, Qingyang Wu, and Yong Jae Lee. 2023. Visual instruction tuning. In *Proceedings of the 37th International Conference on Neural Information Processing Systems (New Orleans, LA, USA) (NIPS '23)*. Curran Associates Inc., Red Hook, NY, USA, Article 1516, 25 pages.
- [21] Qidong Liu, Xian Wu, Wanyu Wang, Yejing Wang, Yuanshao Zhu, Xiangyu Zhao, Feng Tian, and Yefeng Zheng. 2025. LLMEmb: large language model can be a good embedding generator for sequential recommendation. In *Proceedings of the Thirty-Ninth AAAI Conference on Artificial Intelligence and Thirty-Seventh Conference on Innovative Applications of Artificial Intelligence and Fifteenth Symposium on Educational Advances in Artificial Intelligence (AAAI'25/IAAI'25/EAAI'25)*. AAAI Press, Article 1354, 9 pages. doi:10.1609/aaai.v39i1.133327
- [22] Lajanugen Logeswaran and Honglak Lee. 2018. An efficient framework for learning sentence representations. In *International Conference on Learning Representations*.
- [23] Ilya Loshchilov and Frank Hutter. 2017. Decoupled weight decay regularization. *arXiv preprint arXiv:1711.05101* (2017).
- [24] Julian McAuley, Christopher Targett, Qinfeng Shi, and Anton Van Den Hengel. 2015. Image-based recommendations on styles and substitutes. In *Proceedings of the 38th international ACM SIGIR conference on research and development in information retrieval*. 43–52.
- [25] Junhyun Nam, Hyuntak Cha, Sungsoo Ahn, Jaeho Lee, and Jinwoo Shin. 2020. Learning from failure: De-biasing classifier from biased classifier. *Advances in Neural Information Processing Systems* 33 (2020), 20673–20684.
- [26] Aaron van den Oord, Yazhe Li, and Oriol Vinyals. 2018. Representation learning with contrastive predictive coding. *arXiv preprint arXiv:1807.03748* (2018).
- [27] Claudio Pomo, Matteo Attimonelli, Danilo Danese, Fedelucio Narducci, and Tommaso Di Noia. 2025. Do Recommender Systems Really Leverage Multimodal Content? A Comprehensive Analysis on Multimodal Representations for Recommendation. In *Proceedings of the 34th ACM International Conference on Information and Knowledge Management (Seoul, Republic of Korea) (CIKM '25)*. Association for Computing Machinery, New York, NY, USA, 2377–2387. doi:10.1145/3746252.3761398
- [28] Ruihong Qiu, Zi Huang, Hongzhi Yin, and Zijian Wang. 2022. Contrastive learning for representation degeneration problem in sequential recommendation. In *Proceedings of the fifteenth ACM international conference on web search and data mining*. 813–823.
- [29] A Yang Qwen, Baosong Yang, Beichen Zhang, Binyuan Hui, Bo Zheng, Bowen Yu, Chengpeng Li, Dayiheng Liu, Fei Huang, Haoran Wei, et al. 2024. Qwen2.5 technical report. *arXiv preprint* (2024).
- [30] Alec Radford, Jong Wook Kim, Chris Hallacy, Aditya Ramesh, Gabriel Goh, Sandhini Agarwal, Girish Sastry, Amanda Askell, Pamela Mishkin, Jack Clark, et al. 2021. Learning transferable visual models from natural language supervision. In *International conference on machine learning*. PmlR, 8748–8763.

- [31] Ruiyang Ren, Zhaoyang Liu, Yaliang Li, Wayne Xin Zhao, Hui Wang, Bolin Ding, and Ji-Rong Wen. 2020. Sequential recommendation with self-attentive multi-adversarial network. In *Proceedings of the 43rd international ACM SIGIR conference on research and development in information retrieval*. 89–98.
- [32] Simon Schrodli, David T Hoffmann, Max Argus, Volker Fischer, and Thomas Brox. 2024. Two effects, one trigger: On the modality gap, object bias, and information imbalance in contrastive vision-language representation learning. *arXiv preprint arXiv:2404.07983* (2024).
- [33] Peiyang Shi, Michael C Welle, Mårten Björkman, and Danica Kragic. 2023. Towards understanding the modality gap in clip. In *ICLR 2023 workshop on multi-modal representation learning: perks and pitfalls*.
- [34] Mong Yuan Sim, Wei Emma Zhang, Xiang Dai, and Biaoyan Fang. 2025. Can vllms actually see and read? a survey on modality collapse in vision-language models. In *Findings of the Association for Computational Linguistics: ACL 2025*. 24452–24470.
- [35] Fei Sun, Jun Liu, Jian Wu, Changhua Pei, Xiao Lin, Wenwu Ou, and Peng Jiang. 2019. BERT4Rec: Sequential recommendation with bidirectional encoder representations from transformer. In *Proceedings of the 28th ACM international conference on information and knowledge management*. 1441–1450.
- [36] Chongyang Tao, Tao Shen, Shen Gao, Junshuo Zhang, Zhen Li, Kai Hua, Wenpeng Hu, Zhengwei Tao, and Shuai Ma. 2024. Llm are also effective embedding models: An in-depth overview. *arXiv preprint arXiv:2412.12591* (2024).
- [37] Jinpeng Wang, Ziyun Zeng, Yunxiao Wang, Yuting Wang, Xingyu Lu, Tianxiang Li, Jun Yuan, Rui Zhang, Hai-Tao Zheng, and Shu-Tao Xia. 2023. Missrec: Pre-training and transferring multi-modal interest-aware sequence representation for recommendation. In *Proceedings of the 31st ACM International Conference on Multimedia*. 6548–6557.
- [38] Liang Wang, Nan Yang, Xiaolong Huang, Linjun Yang, Rangan Majumder, and Furu Wei. 2024. Improving text embeddings with large language models. In *Proceedings of the 62nd Annual Meeting of the Association for Computational Linguistics (Volume 1: Long Papers)*. 11897–11916.
- [39] Tongzhou Wang and Phillip Isola. 2020. Understanding contrastive representation learning through alignment and uniformity on the hypersphere. In *International conference on machine learning*. PMLR, 9929–9939.
- [40] Weiyao Wang, Du Tran, and Matt Feiszli. 2020. What makes training multi-modal classification networks hard?. In *Proceedings of the IEEE/CVF conference on computer vision and pattern recognition*. 12695–12705.
- [41] Yuling Wang, Changxin Tian, Binbin Hu, Yanhua Yu, Ziqi Liu, Zhiqiang Zhang, Jun Zhou, Liang Pang, and Xiao Wang. 2024. Can small language models be good reasoners for sequential recommendation?. In *Proceedings of the ACM Web Conference 2024*. 3876–3887.
- [42] Nan Wu, Stanislaw Jastrzebski, Kyunghyun Cho, and Krzysztof J Geras. 2022. Characterizing and overcoming the greedy nature of learning in multi-modal deep neural networks. In *International Conference on Machine Learning*. PMLR, 24043–24055.
- [43] Zheng Yuan, Fajie Yuan, Yu Song, Youhua Li, Junchen Fu, Fei Yang, Yunzhu Pan, and Yongxin Ni. 2023. Where to go next for recommender systems? id-vs. modality-based recommender models revisited. In *Proceedings of the 46th International ACM SIGIR Conference on Research and Development in Information Retrieval*. 2639–2649.
- [44] Chao Zhang, Haoxin Zhang, Shiwei Wu, Di Wu, Tong Xu, Xiangyu Zhao, Yan Gao, Yao Hu, and Enhong Chen. 2025. NoteLLM-2: Multimodal Large Representation Models for Recommendation. In *Proceedings of the 31st ACM SIGKDD Conference on Knowledge Discovery and Data Mining V.1 (Toronto ON, Canada) (KDD '25)*. Association for Computing Machinery, New York, NY, USA, 2815–2826. doi:10.1145/3690624.3709440
- [45] Shengzhe Zhang, Liyi Chen, Dazhong Shen, Chao Wang, and Hui Xiong. 2025. Hierarchical Time-Aware Mixture of Experts for Multi-Modal Sequential Recommendation. In *Proceedings of the ACM on Web Conference 2025*. 3672–3682.
- [46] Yuhui Zhang, Jeff Z HaoChen, Shih-Cheng Huang, Kuan-Chieh Wang, James Zou, and Serena Yeung. 2023. Diagnosing and rectifying vision models using language. *arXiv preprint arXiv:2302.04269* (2023).
- [47] Kun Zhou, Hui Wang, Wayne Xin Zhao, Yutao Zhu, Sirui Wang, Fuzheng Zhang, Zhongyuan Wang, and Ji-Rong Wen. 2020. S3-rec: Self-supervised learning for sequential recommendation with mutual information maximization. In *Proceedings of the 29th ACM international conference on information & knowledge management*. 1893–1902.
- [48] Kun Zhou, Hui Yu, Wayne Xin Zhao, and Ji-Rong Wen. 2022. Filter-enhanced MLP is all you need for sequential recommendation. In *Proceedings of the ACM web conference 2022*. 2388–2399.
- [49] Jinguo Zhu, Weiyun Wang, Zhe Chen, Zhaoyang Liu, Shenglong Ye, Lixin Gu, Hao Tian, Yuchen Duan, Weijie Su, Jie Shao, et al. 2025. Internvl3: Exploring advanced training and test-time recipes for open-source multimodal models. *arXiv preprint arXiv:2504.10479* (2025).